Supplementary Information (SI) for Materials Horizons.

Supplementary Information for

Retaining superior electrochromic performance by effective suppression of ion trapping upon cycling

Renfu Zhang[1,3], Qingjiao Huang[1,3], Zhexuan Ou[1], Tooba Afaq Khan[1], Menghan Yin[1], Er Gao[1], Jiawei Sun[1], Rui-Tao Wen[1, 2] *

[1]Department of Materials Science and Engineering, Southern University of Science and Technology, Shenzhen 518055, China

[2]Guangdong Provincial Key Laboratory of Functional Oxide Materials and Devices, Southern University of Science and Technology, Shenzhen, 518055, China

[3]Equally contributed

*Corresponding author: wenrt@sustech.edu.cn

This file includes:

Supplementary Figures 1 to 10

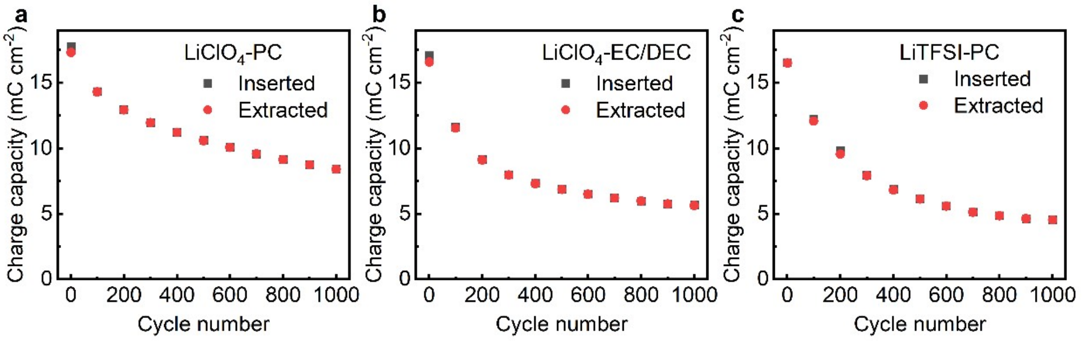

Fig. S1 Charge capacities of *a*-WO_3 films cycling in different electrolytes within 2.0- 4.0 V *vs.* Li/Li^+. **a**, $LiClO_4$-PC. **b**, $LiClO_4$-EC/DEC. **c**, LiTFSI-PC. The concentration of the electrolyte was kept to be 1 mol L^{-1}.

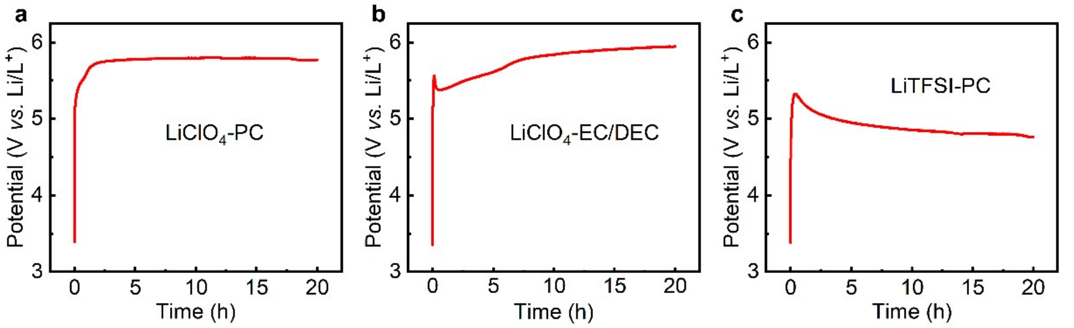

Fig. S2 Potential profiles during the detrapping processes of *a*-WO_3 films in different electrolytes. **a**, $LiClO_4$-PC. **b**, $LiClO_4$-ECDEC. **c**, LiTFSI-PC. The constant current was set to be 3μm cm^{-2} in all electrolytes.

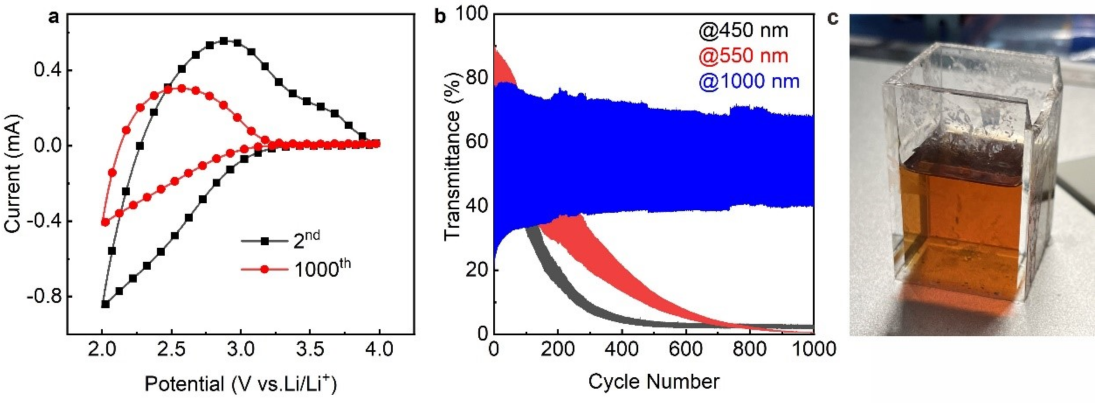

Fig. S3 The electrochromic performance of *a*-WO_3 film under cycling within the electrolyte of $LiClO_4$-DEC. **a**, CV curves and **b**, *in -situ* transmittance variation at specific wavelengths of WO_3 during cycling in $LiClO_4$-DEC were recorded. **c**, The color of the $LiClO_4$-DEC electrolyte after electrochemical cycling. The $LiClO_4$-DEC electrolyte underwent a color change from its initial transparency to orange as a result of a side reaction between the DEC solvent and the lithium sheet electrode.[1] The color alteration of the electrolyte indicates its deterioration and can not be used as an electrolyte alone in our study.

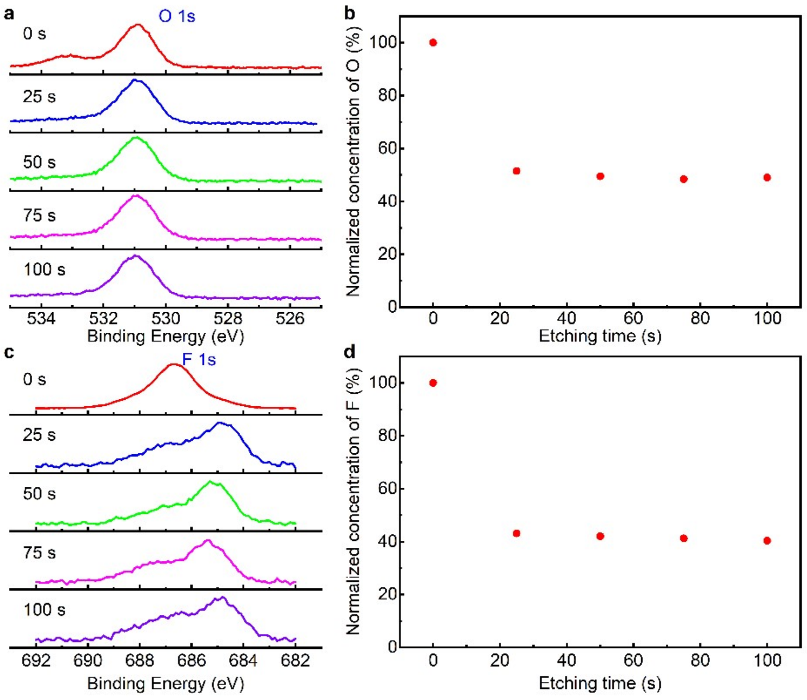

Fig. S4 XPS results of *a*-WO$_3$ films after cycling in different electrolytes. **a**, XPS depth profiles and **b**, corresponding normalized concentrations of O concentration of the *a*-WO$_3$ film cycling in LiClO$_4$-EC/DEC. **c**, XPS depth profiles and **d**, corresponding normalized concentrations of F concentration of the *a*-WO$_3$ film cycling in LiTFSI-PC.

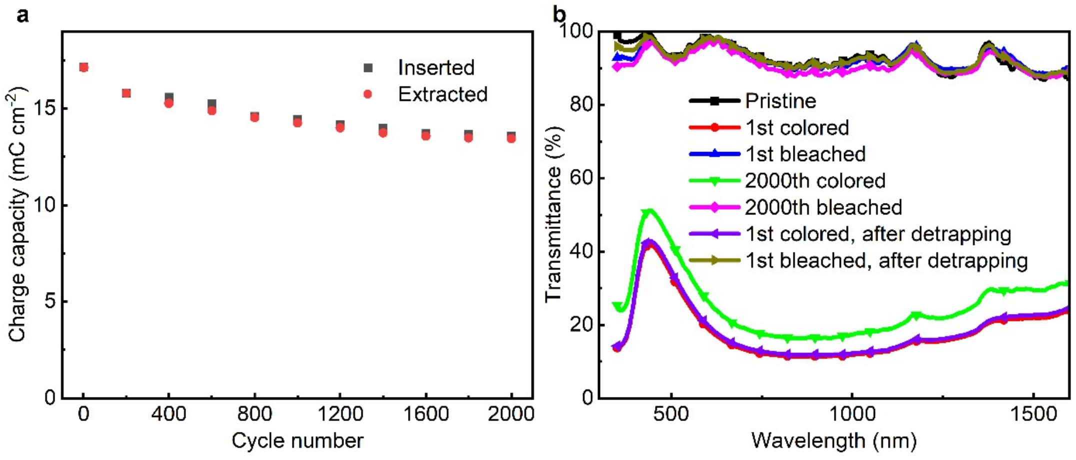

Fig. S5 Electrochromic performance of the *a*-WO$_3$ film cycling in the electrolyte of 1M LiOTF-PC. **a**, Charge capacities of the *a*-WO$_3$ film upon cycling. **b**, *In-situ* optical transmittances @ 350-1600 nm of the *a*-WO$_3$ film at different states.

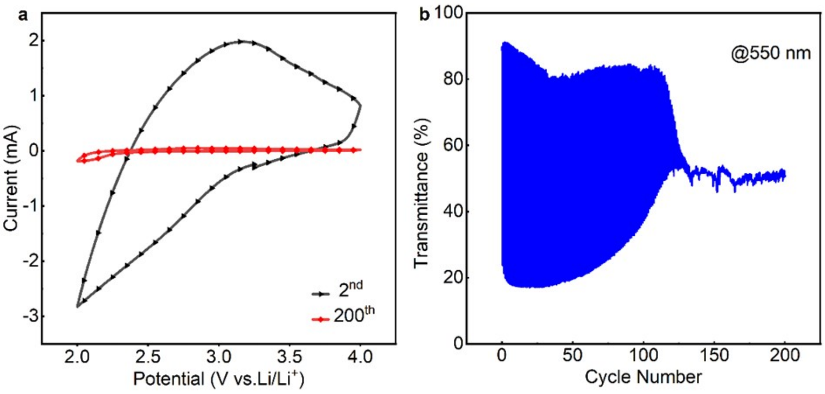

Fig. S6 Electrochromic performance of the *a*-WO_3 film cycling in the electrolyte of 1M $LiPF_6$-PC. a, CV curves and **b**, *in-situ* transmittance variations monitored upon cycling. The severe degradation of the *a*-WO_3 film within $LiPF_6$-PC can be discerned. The rapid attenuation of *a*-WO_3 in the $LiPF_6$-PC solution is attributed to the fact that Li^+ has a relatively large charge-to-radius ratio, it can easily separate fluorine from hexafluorophosphate (PF_6^-). Therefore, the ion-paired $LiPF_6$ can be easily decomposed into phosphorus pentafluoride (PF_5) and lithium fluoride (LiF) when it is not completely dissociated.[2] The generated PF_5 not only catalyzes the ring-opening reaction of cyclic carbonates to form carbonate polymers at the interface [2,3], but also reacts with trace amounts of water to produce aggressive hydrogen fluoride (HF). This HF will damage the integrity of the interface and subsequently trigger a variety of parasitic side reactions[4].

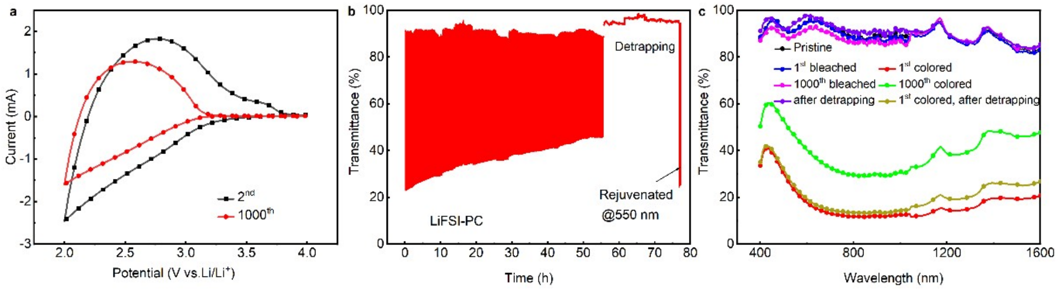

Fig. S7 Electrochemical results and optical spectral of *a*-WO_3 film cycling and rejuvenation in 1M LiFSI-PC. a to **c**, CV curves, *In-situ* optical transmittances profiles of single wavelength at 550 nm and of full spectrum @ 350-1600 nm of the *a*-WO_3 film upon cycling and detrapping in the electrolyte of LiFSI-PC.

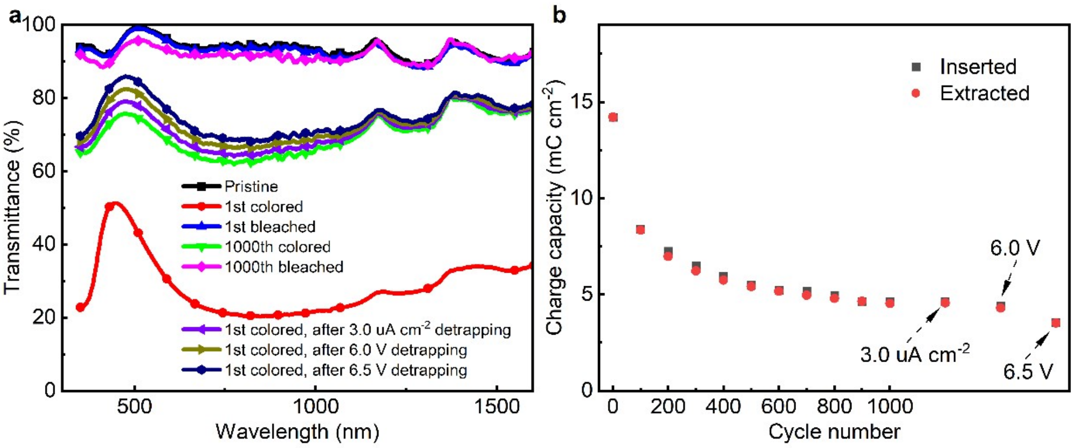

Fig. S8 Optical spectral and electrochemical results of the *a*-WO_3 film cycling and detrapping in the 1M LiTFSI-PC electrolyte. **a**, *In-situ* optical transmittances @ 350- 1600 nm of the *a*-WO_3 film at different states. **b**, Charge capacities of the *a*-WO_3 film while cycling and detrapping in the LiTFSI-PC electrolyte.

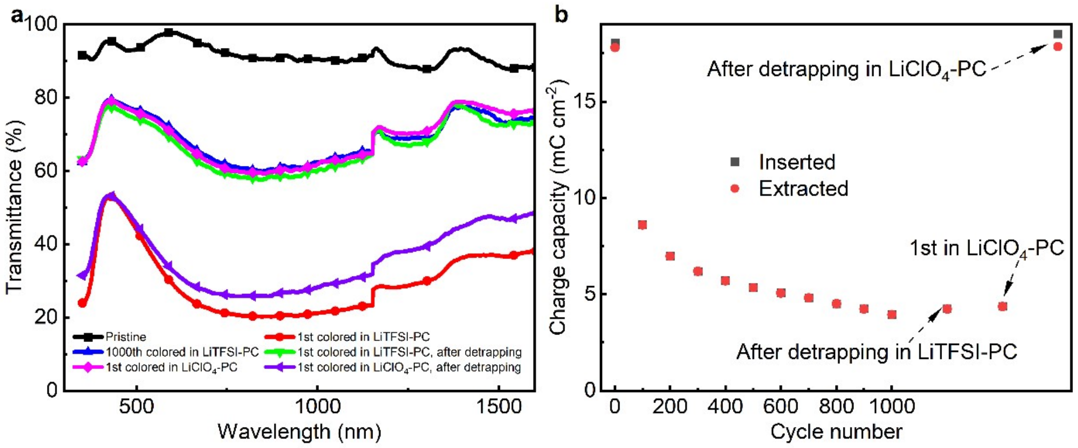

Fig. S9 Optical spectral and electrochemical results of the *a*-WO$_3$ film cycling and detrapping in the LiTFSI-PC and the LiClO$_4$-PC electrolyte. **a**, *In-situ* optical transmittances @ 350- 1600 nm of the a-WO$_3$ film at different states as marked. **b**, Charge capacities of the *a*-WO$_3$ film while cycling and detrapping in the LiTFSI-PC and the LiClO$_4$-PC electrolyte.

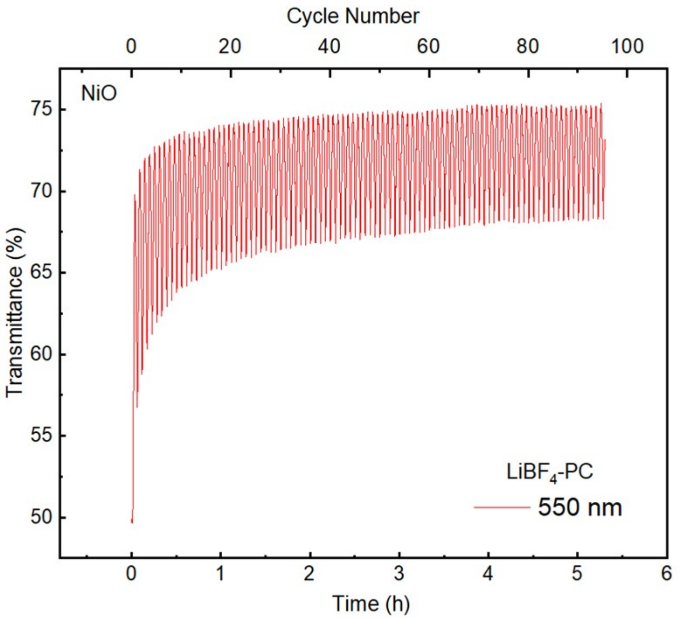

Fig. S10 NiO cycling in LiBF$_4$-PC, showing an activation. The potential window is 2.0-4.0 V vs Li, and the sweep rate is 20 mV s^{-1}, which is kept to the same for a-WO$_3$.

References

1 Wang, Y. *et al.* Electrolyte-Mediated Misconception of Carbon-Based Electrode Performance and Beyond in Metal-Ion Batteries. *Adv. Energy Mater.*, **13**, 2301354 (2023).

2 Han, J. G., Kim, K., Lee, Y. & Choi, N. S. Scavenging materials to stabilize LiPF6-containing carbonate-based electrolytes for Li-ion batteries. *Adv. Mater.*, **31**, 1804822 (2019).

3 Sloop, S. E., Kerr, J. B. & Kinoshita, K. The role of Li-ion battery electrolyte reactivity in performance decline and self-discharge. *J. Power Sources* **119**, 330-337 (2003).

4 Goodenough, J. B. & Kim, Y. Challenges for rechargeable Li batteries. *Chem. Mater.*, **22**, 587-603 (2010).